The EMBO Journal Vol.17 No.14 pp.3899–3908, 1998

A matrix-less measles virus is infectious and elicits extensive cell fusion: consequences for propagation in the brain

Toni Cathomen[1], Branka Mrkic, Danièle Spehner[2], Robert Drillien[2], Roland Naef[3], Jovan Pavlovic[4], Adriano Aguzzi[5], Martin A.Billeter and Roberto Cattaneo[6]

Institut für Molekularbiologie, Abt. I, Universität Zürich, Hönggerberg, 8093 Zürich, [3]Institute of Cell Biology, Swiss Federal Institute of Technology, Zürich, [4]Institut für Medizinische Virologie, [5]Institut für Neuropathologie, Universität Zürich, Zürich, Switzerland and [2]Etablissement de Transfusion Sanguine de Strasbourg, Strasbourg, France

[1]Present address: Laboratory of Genetics, The Salk Institute, San Diego, CA, USA

[6]Corresponding author
e-mail: cattaneo@molbio1.unizh.ch

Measles viruses (MV) can be isolated from the brains of deceased subacute sclerosing panencephalitis patients only in a cell-associated form. These viruses are often defective in the matrix (M) protein and always seem to have an altered fusion protein cytoplasmic tail. We reconstituted a cell-free, infectious M-less MV (MV-ΔM) from cDNA. In comparison with standard MV, MV-ΔM was considerably more efficient at inducing cell-to-cell fusion but virus titres were reduced ~250-fold. In MV-ΔM-induced syncytia the ribonucleocapsids and glycoproteins largely lost co-localization, confirming the role of M protein as the virus assembly organizer. Genetically modified mice were inoculated with MV-ΔM or with another highly fusogenic virus bearing glycoproteins with shortened cytoplasmic tails (MV-Δ_{tails}). MV-ΔM and MV-Δ_{tails} lost acute pathogenicity but penetrated more deeply into the brain parenchyma than standard MV. We suggest that enhanced cell fusion may also favour the propagation of mutated, assembly-defective MV in human brains.

Keywords: cell-to-cell fusion/envelope protein cytoplasmic tail/matrix protein/subacute sclerosing panencephalitis/virus assembly

Introduction

Subacute sclerosing panencephalitis (SSPE) is one of the most thoroughly studied neurodegenerative diseases caused by persistent viral infection of the human central nervous system (CNS), and serves as a model for the analysis of persistent viral infections causing other human syndromes (Kristensson and Norrby, 1986). SSPE generally develops 5–10 years after acute measles virus (MV) infection, starting with subtle intellectual and psychological dysfunction and progressing to motor and sensory deterioration, cerebral degeneration and death within months or years (ter Meulen *et al*., 1983). MV is a non-integrating negative-strand RNA virus which consists of a replicative unit, the ribonucleocapsid and an envelope. The envelope contains two integral membrane proteins, fusion (F) and haemagglutinin (H), and a membrane-associated matrix (M) protein that contacts the ribonucleocapsid (Hirano *et al*., 1993), as well as the cytoplasmic tail of the F protein (Cathomen *et al*., 1998; Spielhofer *et al*., 1998).

A typical SSPE feature is the failure of persistently infected brain cells to produce progeny virus particles (ter Meulen *et al.*, 1983). Since defects in M are very common in SSPE (Cattaneo *et al*., 1988) and M-defective MV genomes expand clonally in the CNS (Baczko *et al*., 1993), it has been postulated that M is dispensable for virus replication and spread in human brain, and that abrogation of M protein function accounts for lack of particle formation and may favour virus persistence. More recently, it has been shown that the cytoplasmic tail of the F protein is altered in all SSPE viruses analysed so far (Schmid *et al*., 1992). This suggests that a common prerequisite for SSPE may not be solely the loss of M protein function, but more generally any alteration interfering with envelope assembly (Billeter and Cattaneo, 1991; Griffin and Bellini, 1996). Recently, it has been shown that engineered MVs with altered F and H glycoprotein cytoplasmic tails gain cell-to-cell fusion competence (Cathomen *et al.*, 1998), suggesting that these interactions may be involved not only in virus assembly, but also in virus-induced cell fusion.

Taken together, these observations suggest links between loss of proper MV particle assembly and extensive cell fusion, virus spread in the CNS and brain pathogenesis. Up until now, the mechanisms connecting these events could not be tested experimentally for two reasons. First, M-defective, cell-free virus was not available. Secondly, comparative analysis of the neuropathogenesis of different MV strains was possible only in primates (van Binnendijk *et al*., 1995), as newborn rodents were susceptible only to neuroadapted MV (Liebert and Finke, 1995). Recently, however, newborn mice expressing the main MV receptor CD46 in neural cells (Rall *et al*., 1997) and adult animals expressing CD46 with human-like tissue specificity and defective for the interferon type I receptor (Mrkic *et al*., 1998) were found to support the brain spread of neurotropic as well as attenuated MV strains.

An M-less MV (MV-ΔM) was generated here using a modified cDNA copy of the negative-strand RNA genome of the Edmonston B vaccine strain (Radecke *et al*., 1995). The propagation of this virus was compared with that of the standard (Edmonston) MV in cultured cells. Moreover, the spread and pathogenesis of the M-less MV, the standard MV and a virus bearing F and H proteins with shortened cytoplasmic tails was analysed after intracerebral inoculation of genetically modified mice (Mrkic *et al*., 1998).

© Oxford University Press

Results

An M-less MV is infectious and highly fusogenic

In an attempt to generate an M-less virus, an MV antigenomic cDNA, p(+)MV-ΔM, was constructed that contained a 960 nucleotide deletion in the M-coding region (Figure 1A, centre). Plasmid p(+)MV-ΔM and the control plasmid p(+)MV (Figure 1A, top), which gives rise to a standard sequence-tagged Edmonston B MV, were used in separate experiments to transfect the helper cell line 293-3-46 (Radecke *et al*., 1995). After 3–5 days syncytia were observed, suggesting rescue of infectivity.

The identity of this infectivity was verified by M-gene-specific reverse transcription–PCR (RT–PCR) (Figure 1B). The DNA amplification product obtained from MV-ΔM-infected cells was 960 nucleotides shorter than that obtained from standard MV-infected cells (Figure 1B, compare lane 6 with lane 3) and was the same size as the control product derived from the p(+)MV-ΔM DNA (Figure 1B, lane 4). In both cases, a control amplification over the N gene yielded the expected 475 nucleotide fragment (Figure 1B, lanes 9 and 12). When reverse transcriptase was omitted from the reactions (Figure 1B, lanes 2, 5, 8 and 11), no product could be detected indicating that the DNA products obtained in lanes 3, 6, 9 and 12 were not due to amplification from the remaining cDNA plasmids but to amplification from an RNA template.

To further characterize the infection, protein extracts of ^{35}S-methionine pulse-labelled MV-ΔM-infected, MV-infected or mock-infected Vero cells were immunoprecipitated with an anti-MV antibody and separated by gel electrophoresis (Figure 1C). The viral H and nucleocapsid (N) proteins were monitored in both cells infected with MV (Figure 1C, lane 3) and with MV-ΔM (Figure 1C, lane 7), and only standard MV-infected cells (Figure 1C, lane 3) but not MV-ΔM-infected cells (Figure 1C, lane 7) produced M protein.

Since M protein may bridge the encapsidated viral RNA genomes with the two integral membrane proteins H and F, it may also influence their transport within the infected cell. Intracellular transport was analysed by comparing the glycosylation state of the H protein in MV-infected cells with that in MV-ΔM-infected cells, immediately or 4 h after 1 h pulse-labelling. In both MV-infected cells (Figure 1C, lanes 5 and 6) and MV-ΔM-infected cells (Figure 1C, lanes 9 and 10) a large fraction of the H protein became partially endo H resistant 4 h after synthesis (Figure 1C, triangles in lanes 6 and 10), suggesting passage through the *medial*-Golgi. The H protein intracellular transport is therefore influenced only slightly, if at all, by the absence of M-protein expression.

Microscopic observation of infected cells revealed that at any given time the MV-ΔM syncytia were considerably larger than the standard MV syncytia (Figure 2A–F; for two average syncytia). In standard MV infections numerous secondary infection centres formed starting at day 3 (Figure 2B and C, arrows), whereas in MV-ΔM infections secondary syncytia were very rare (Figure 2F, arrowhead). Quantification of the extent of cell fusion after infection with a multiplicity

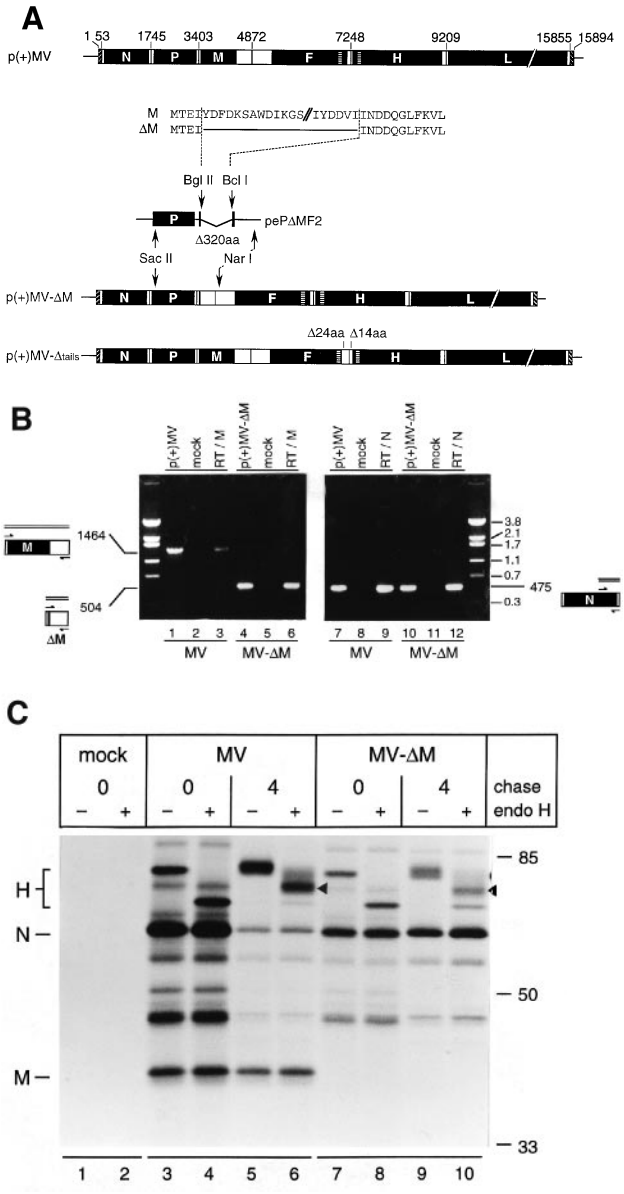

Fig. 1. Generation and analysis of an M-less MV. (**A**) Structure of MV antigenomic cDNAs encoding standard (top) or mutant (bottom) viruses. The MV genomes of plasmid p(+)MV (Radecke *et al*., 1995), p(+)MV-ΔM and p(+)MV-Δ_{tails} are shown. The black boxes represent the reading frames of the six MV cistrons N, P, M, F, H and L. The structure of the subcloning intermediate pePΔMF2 is depicted with the relevant restriction enzyme sites (centre) and the predicted protein sequence of M and ΔM proteins above it. For M, only the terminal amino acids are indicated. Nucleotide numbering is according to DDBJ/EMBL/GenBank accession No. Z66517. aa, amino acids. (**B**) RT–PCR analysis of MV and MV-ΔM virus genomes. Template RNAs for the amplifications shown in lanes 2, 3, 8 and 9 were from MV-infected cells, template RNAs for the amplifications shown in lanes 5, 6, 11 and 12 were from MV-ΔM-infected cells. Reverse transcriptase was omitted in the reactions of lanes 2, 5, 8 and 11 (mock). A control reaction based on plasmid DNA is shown in lanes 1, 4, 7 and 10. On the left the M and ΔM genes and on the right the N gene, respectively, are shown schematically with the amplification primers. (**C**) Immunoprecipitation of pulse-labelled MV proteins from MV- and MV-ΔM-infected cells. Proteins in lanes 1 and 2 were precipitated from mock-infected Vero cells, in lanes 3–6 from MV-infected cells and in lanes 7–10 from MV-ΔM-infected cells. The presence (+) or absence (–) of endo H in the glycosidase digestion and the length of the chase time (0 or 4 h) are indicated on the top. The positions of H, N and M proteins are indicated on the left, the size markers are on the right.

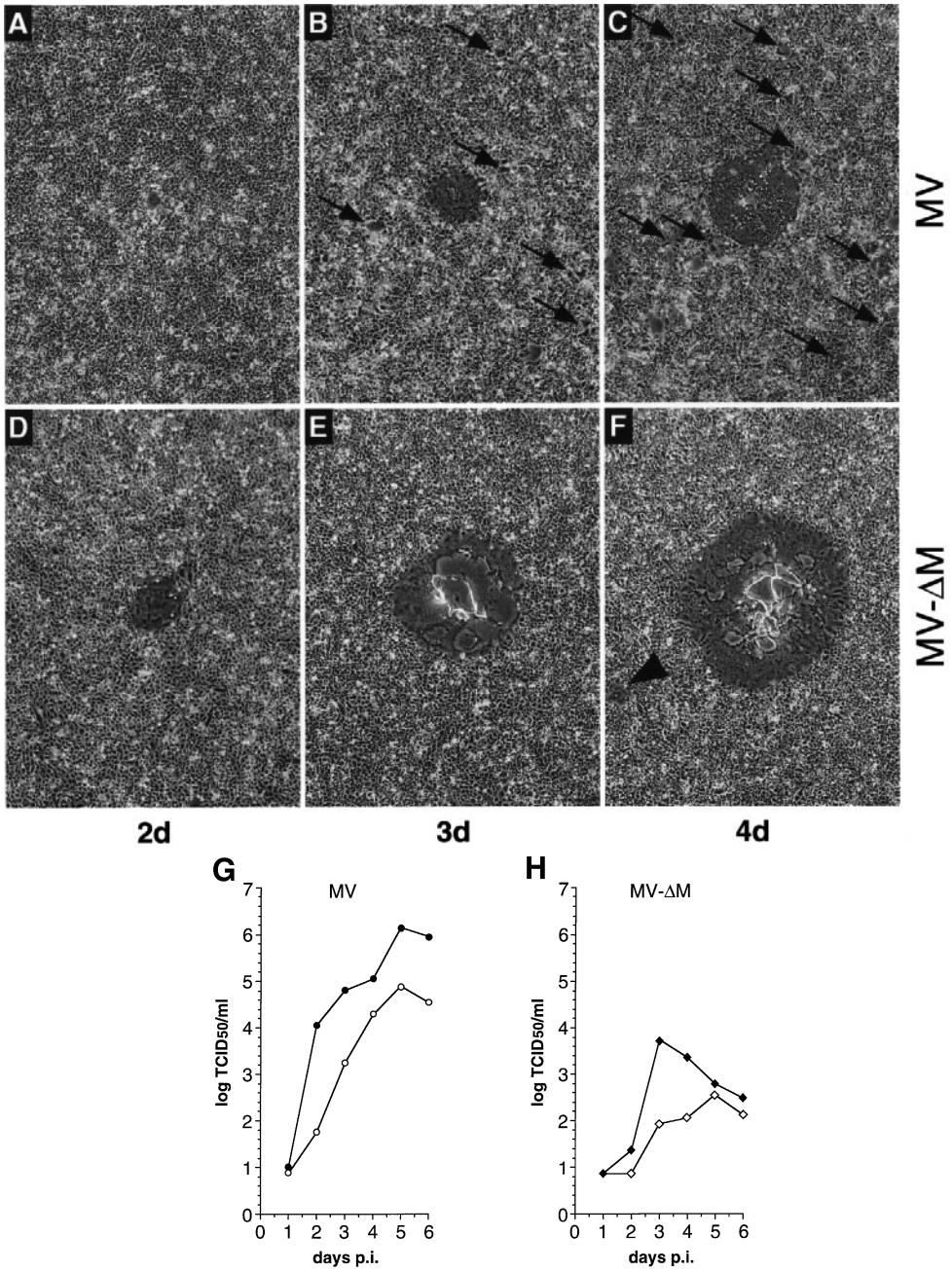

Fig. 2. Characteristics of MV-ΔM infection of Vero cells. (**A**–**F**) Syncytia growth on MV- or MV-ΔM-infected Vero cells. After infection with an m.o.i. of 0.001, MV-induced syncytia (A–C) and MV-ΔM-induced syncytia (D–F) were monitored by phase-contrast microscopy at 2 days (A, D), 3 days (B, E) and 4 days (C, F) p.i. The arrows (B, C) and arrowhead (F) indicate secondary infection centres. (**G**, **H**) Time course of virus production of MV-infected or MV-ΔM-infected Vero cells. After infection with an m.o.i. of 0.01 virus titres were determined by 50% end-point dilution at the indicated time points. The titre of cell-associated infectivity is indicated by solid circles (G, MV) or diamonds (H, MV-ΔM), and that of released virus by open circles or diamonds, respectively. The average of two independent experiments is shown. $TCID_{50}$, tissue culture infectious dose 50; p.i. post-infection.

of infection (m.o.i.) of 0.01 revealed that after 4 days ~75% of the nuclei of an MV-ΔM-infected cell monolayer were in syncytia, compared with ~25% of the nuclei of MV-infected cells. After 6 days, >90% of the cells were involved in syncytia in both MV and MV-ΔM infections, and cell mortality was substantial. These data indicate that the M-less virus is more efficient than standard MV at inducing cell-to-cell fusion; at later stages, the formation of secondary infectious centres allows standard MV to compensate for the initial delay.

An M-less MV is assembly defective

The production of infectivity was then followed after inoculating Vero cells with an m.o.i. of 0.01. Both cell-associated and supernatant infectivity were measured at 1 day intervals. The growth curves indicated that MV-ΔM infections (Figure 2H) produced a maximum of 5500 tissue culture infectious dose 50 ($TCID_{50}$)/ml 3 days after infection. Cell-free infectivity reached a maximum of 360 $TCID_{50}$/ml 5 days after infection. In the parallel standard MV infections (Figure 2G) the titres of cell-associated

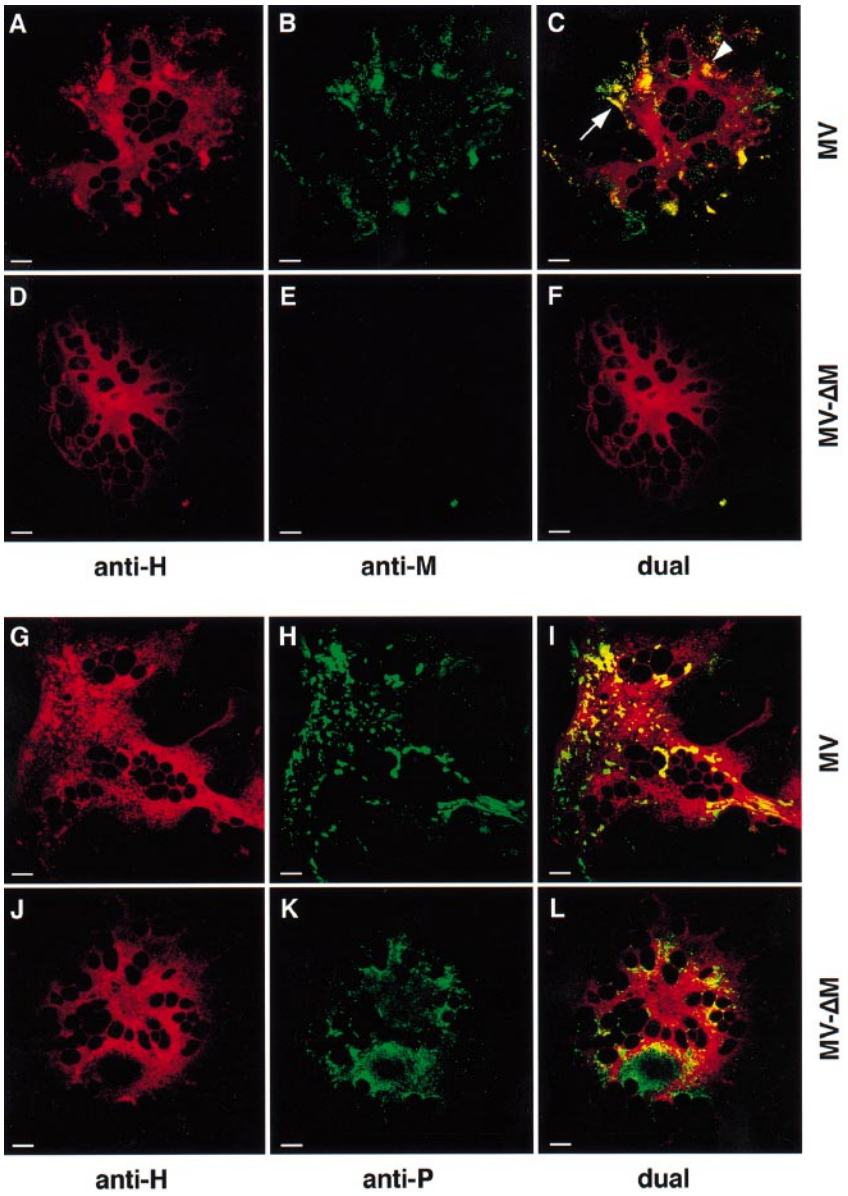

Fig. 3. Distribution of viral proteins in infected Vero cells. Two to three days after infection cells were permeabilized and stained with H-, M- or P-specific antibodies. Immunoreactivity was detected by confocal microscopy. Each micrograph represents a 0.4 μm optical section of syncytia found after infection with MV (**A**–**C**, **G**–**I**) or MV-ΔM (**D**–**F**, **J**–**L**). Images show the localization of H protein in red (A, D, G, J), and of M (B, E) or P protein (H, K) in green. In superimposed pictures co-localization of two proteins is displayed in yellow (C, F, I, L). In (C) putative assembly sites situated intracellularly (arrowhead) or below the cell surface (arrow) are indicated. The bars represent 20 μm.

and cell-free virus peaked 5 days post-infection (p.i.) at 1.4×10^6 and 8×10^4 $TCID_{50}$/ml, respectively. Thus the ratio of released to cell-associated infectivity was similarly low in standard and MV-ΔM infections, but titres of MV-ΔM were reduced ~250 times. Characterization of released MV-ΔM virus infectivity on sucrose gradients was attempted but failed (see Discussion).

To gain further insight into MV-ΔM infections, the cellular distribution of viral proteins was characterized using confocal microscopy. Syncytia with ~30 nuclei monitored in a standard MV infection (A–C and G–I) or in a MV-ΔM infection (D–F and J–L) are shown in Figure 3. In a standard MV infection the H protein (Figure 3A), the F protein (not shown) and the M protein (Figure 3B) were concentrated in bright patches. Superimposition of the M and H images indicated co-localization of the two proteins in these patches (Figure 3C) as monitored intracellularly (arrowhead) and at the cell surface (arrow). However, in MV-ΔM infections no M protein was produced (Figure 3E) and the H protein was distributed more homogeneously within the cell and on the cell surface (Figure 3D). Similarly, in standard MV infections the H protein (Figure 3G) and the phosphoprotein (P; Figure 3H) or the N protein (not shown), both constituents of the ribonucleocapsid, co-localized in bright patches (Figure 3I). In MV-ΔM infections the P protein was distributed more homogeneously (Figure 3K) and co-localization with the H protein was less frequent (Figure 3L).

The structure of MV- and MV-ΔM-infected cells was also examined at higher resolution by electron microscopy. In Vero cells infected with standard MV, protruding

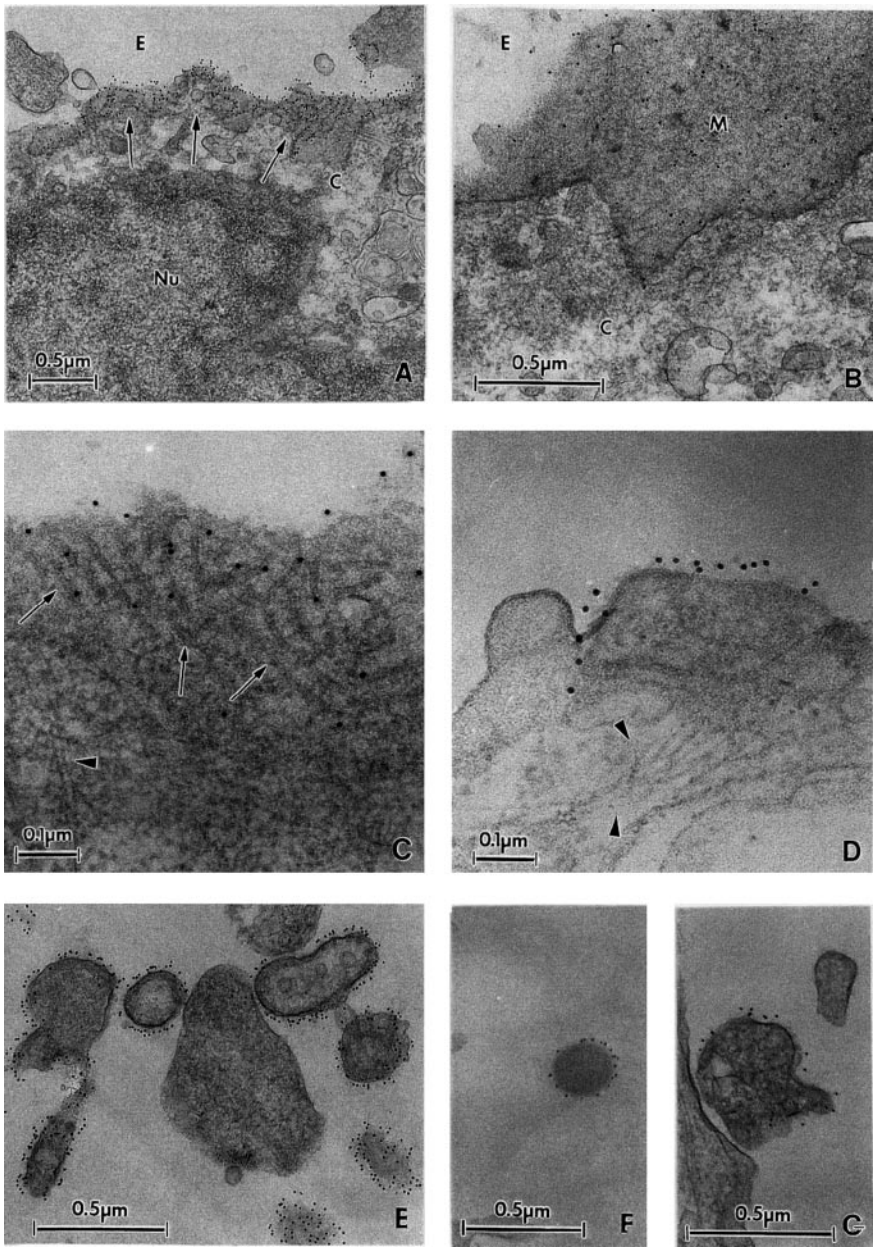

Fig. 4. Electron microscopy of infected Vero cells and viral particles. Vero cells were infected with standard MV (A, C, E) or MV-ΔM (B, D, F, G) with an m.o.i. of 0.05. After 2 days at 32.5°C, F protein (A, B, E) or H protein (C, D, F, G) was detected by indirect immunogold labelling using a pool of F- or H-specific monoclonal antibodies and colloidal-gold-coupled goat anti-mouse antibodies. (**A**–**D**) display characteristic portions of the infected cell surface. The arrows in A and C point to ribonucleocapsid filaments (18 nm thick). The arrowheads in C and D point to filaments of the cytoskeleton. (**E**–**G**) display virus-like particles observed near cells infected with standard MV (E) or with MV-ΔM (F, G). E, extracellular space; C, cytoplasm; Nu, nucleus; M, membrane. The bar length is indicated.

structures enriched with viral envelope proteins (Figure 4A, immunogold-labelled for F protein) were observed frequently along the infected cell surface. Labelling of the viral-glycoprotein-enriched areas often coincided with electron-dense filaments apparent beneath the cell surface. At a higher magnification (Figure 4C, labelling for H protein), 18 nm thick ribonucleocapsid filaments could be visualized clearly within such structures (arrows), indicating that the concentration of the viral glycoproteins is higher in membrane regions overlaying the ribonucleocapsids.

In contrast to MV-infected cells, the surface of cells infected with MV-ΔM did not display characteristic budding particles although dispersed immunogold labelling of the glycoproteins was apparent (Figure 4B and D, labelling for F and H protein, respectively). Moreover, in areas where surface labelling of viral glycoproteins was higher, ribonucleocapsid filaments did not accumulate (Figure 4D) although overall the same amount of viral ribonucleocapsids accumulated in the cytoplasm of cells infected with standard MV or MV-ΔM, respectively (not shown). Only on rare occasions were virus-like particles detected near cells infected with MV-ΔM (Figure 4F and G). Some of these particles (Figure 4F) were reminiscent of standard MV (Figure 4E) considering both their size and the fringe of surface spikes. Most of them, however, could be merely cell fragments that had detached because of cell damage due to the infection (Figure 4G). Taken

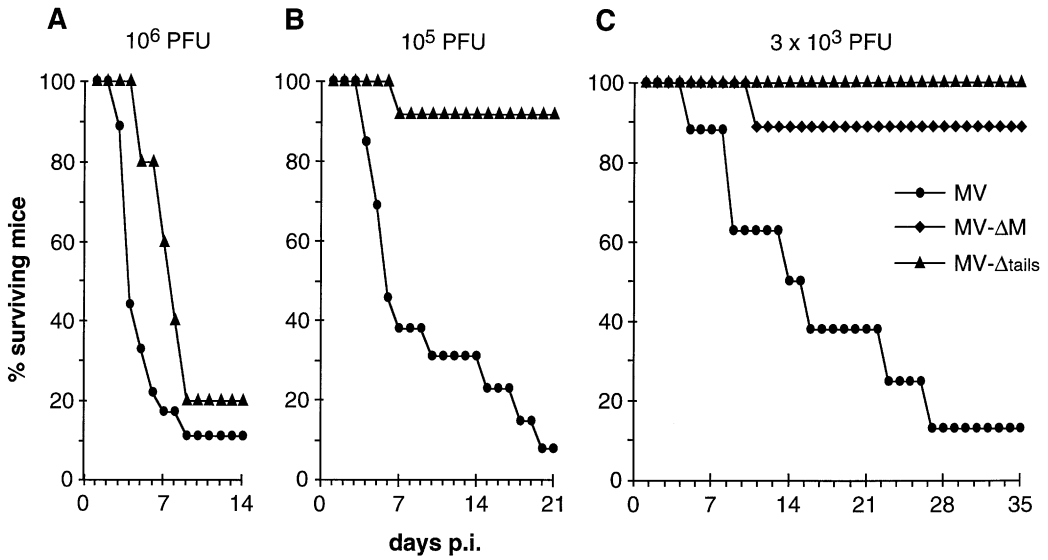

Fig. 5. Mortality of genetically modified mice after MV intracerebral inoculation. Six to eight-week-old genetically modified mice were infected with 10^6 p.f.u. (**A**), 10^5 p.f.u. (**B**) or 3×10^3 p.f.u. (**C**) of standard MV (●), MV-ΔM (◆), or MV-Δ_{tails} (▲). The number of infected animals are: (A) $n = 18$ for MV, $n = 5$ for MV-Δ_{tails}; (B) $n = 13$ for MV, $n = 12$ for MV-Δ_{tails}; (C) $n = 8$ for MV and MV-Δ_{tails}, $n = 9$ for MV-ΔM.

together, the microscopic analyses indicated that the viral glycoproteins and the ribonucleocapsids often co-localize below the plasmalemma in standard MV infections. In MV-ΔM infections the glycoproteins are distributed more homogeneously and ribonucleocapsids do not concentrate below the cell surface.

Brain pathogenesis of highly fusogenic/assembly-defective MV

To ascertain the pathogenic effects of MV-ΔM, we infected intracerebrally 6- to 8-week-old mice expressing the human receptor CD46 and defective for the interferon type I system (Mrkic *et al*., 1998). Since MV-ΔM reached only low titres, we also analysed the pathogenesis of another virus, MV-Δ_{tails} (Figure 1A, bottom), which is partially defective in envelope assembly and highly fusogenic owing to shortened F and H cytoplasmic tails (formerly named MV-HcΔ14/FcΔ24; Cathomen *et al.*, 1998).

No significant difference in the lethality of MV and MV-Δ_{tails} was evident following the inoculation of adult mice with a high dose of virus (10^6 plaque forming units, p.f.u.): ~90% of standard MV-infected animals died 3–9 days p.i., whereas ~80% of MV-Δ_{tails}-infected mice died 5–9 days p.i. (Figure 5A). All affected animals showed clinical signs of neurologic disease: initial hyperactivity followed by mild ataxic gait, hunchback, occasional epileptic seizures, lethargy and death.

When less virus was applied (10^5 p.f.u.; Figure 5B), a difference between MV- and MV-Δ_{tails} infections became apparent: whereas <10% of MV-Δ_{tails}-infected mice died, the mortality for standard MV-infected mice remained ~90%. Inoculation with 3000 p.f.u. confirmed this tendency (Figure 5C): the mortality dropped to 0 for MV-Δ_{tails}-infected animals but seven out of eight standard MV-infected mice died 5–27 days p.i. Similarly, only one of nine animals infected with 3000 p.f.u. of MV-ΔM (the highest dose in a feasible injection volume) died. Surviving animals monitored for up to 8 months p.i. did not show any clinical sign of late neurologic disease. Taken together, these data indicate that assembly-defective MV mutants are less pathogenic than standard MV in an acute brain infection.

To follow the course of brain infection, mice inoculated with 3000 p.f.u. of any of the three above viruses at different times p.i. (3 days to 16 weeks) were sacrificed. Coronal and sagittal brain sections of 24 mouse brains were examined histologically either directly by staining with haematoxylin/eosin (HE) and luxol/nuclear fast red to monitor inflammatory cells and myelin fibres, respectively, or after immunohistochemical processing for glial fibrillary acidic protein (GFAP) to reveal reactive astrocytic gliosis. In addition, brain sections were analysed by *in situ* hybridization using an MV N-mRNA-specific probe.

A selection of the most informative data obtained at 14 days p.i. is shown in Figure 6. Infectious centres were detected in different regions of the brain parenchyma including the frontal part of the cerebrum, the hippocampus, the corpus callosum and the adjacent neocortex, the hypothalamus and the pons. No clearcut difference in the extent of viral replication was monitored in MV-ΔM and standard MV infections since the number of infectious centres detected was limited. In general, strong encephalitis, attested by extensive inflammatory infiltrations (Figure 6D, hypothalamus) and haemorrhage combined with massive gliosis (Figure 6E), became evident at sites of virus replication (Figure 6F, MV-ΔM). Moreover, virus (Figure 6I, standard MV) replicating in myelin-rich areas caused massive inflammation leading to focal demyelination (Figure 6G, corpus callosum) and strong gliosis (Figure 6H).

Besides these common features, important differences were monitored when comparing GFAP-immunostained sections of standard MV-infected mouse brains with MV-ΔM- or MV-Δ_{tails}-infected mouse brains. Whereas neuronal cell loss predominated in the hippocampal pyramidal cell ribbon (CA1 region, extending between the arrowheads in Figure 6B) in all of the four standard

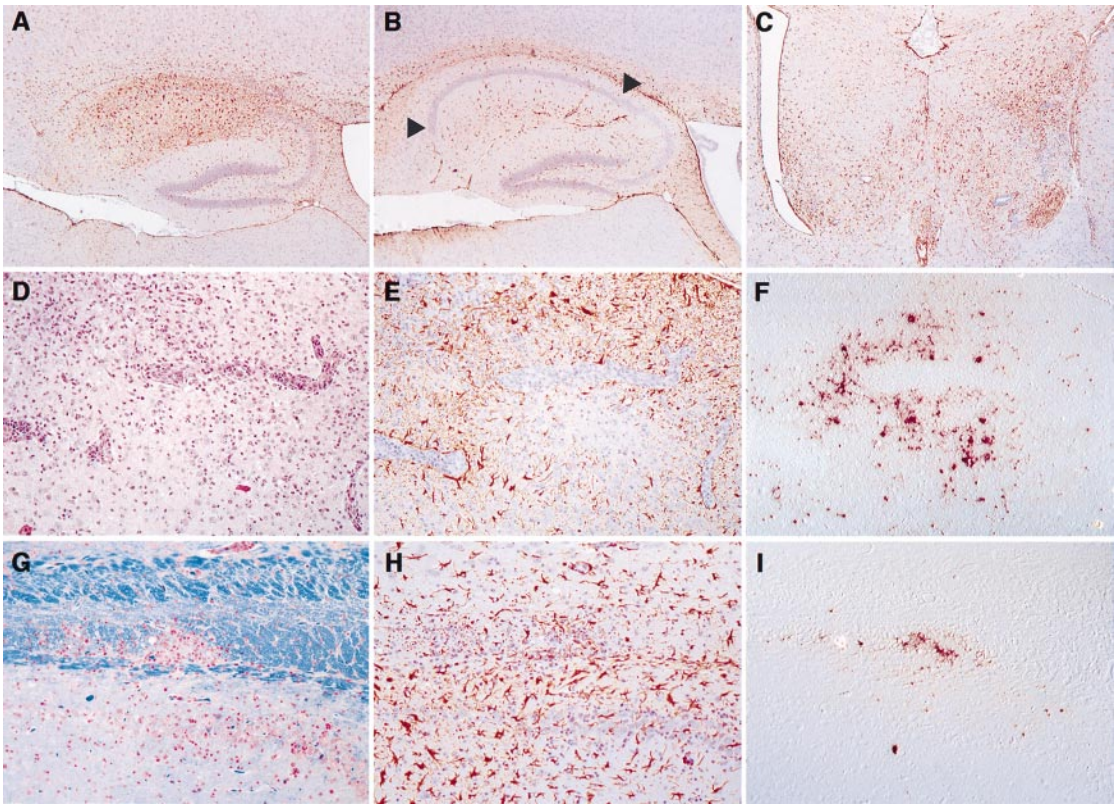

Fig. 6. Histopathological analysis of infected mouse brains. Mice were sacrificed 2 weeks after intracerebral inoculation with 3000 p.f.u. of standard MV (A, G–I), MV-Δ_{tails} (B), or MV-ΔM (C–F). Brain sections were immunostained for GFAP (A–C, E, H), or stained directly with haematoxylin/eosin (D) or luxol/nuclear fast red (G). Virus replication was detected by *in situ* hybridization with an MV N-mRNA-specific probe (F, I). Microphotographs show similar segments of the hippocampus/corpus callosum area of standard MV (**A**, 40×) or MV-Δ_{tails} (**B**, 40×) infected brains and a fragment of the thalamus of an MV-ΔM-infected brain (**C**, 50×). Comparative analysis of an MV-ΔM-infected hypothalamus (D–F, 132×) monitored extensive inflammatory infiltration (**D**) and massive gliosis (**E**) in an area of virus replication (**F**). In myelin-fibre-rich areas (blue staining), as shown for a corpus callosum segment infected with standard MV (G–I, 160×), inflammation in combination with focal demyelination (**G**) and strong gliosis (**H**) were detected in an area of virus replication (**I**).

MV-infected brains analysed (Figure 6A, hippocampus), only one of eight MV-ΔM-infected brains and nought out of six MV-Δ_{tails}-infected brains (Figure 6B) revealed a similar pathology. Rather, in MV-ΔM-infected and MV-Δ_{tails}-infected mice multiple immunoreactive centres were distributed over the whole brain (Figure 6C, thalamus region). Thus these analyses indicated that MV-ΔM and MV-Δ_{tails} lost almost completely, not only pathogenicity (Figure 5), but also the capacity to eliminate specifically cells in the CA1 region of the hippocampal pyramidal ribbon (Figure 6B). Nevertheless, highly fusogenic/assembly-defective MV infections penetrated more deeply into the brain parenchyma than standard virus infections (Figure 6C).

The other data can be summarized as follows: early (3–7 days) brain sections revealed virus replication in combination with multifocal meningitis and mild general inflammation. In addition, limited gliosis was detected in the hippocampus. Later (5 or 16 weeks), only samples from MV-ΔM or MV-Δ_{tails} animals were available, because standard MV-infected mice succumbed. In these samples MV replication was no longer detectable by *in situ* RNA analysis but clinical signs such as cell sclerosis, that is cerebral neuronal degeneration followed by invasion of glial cells and scar tissue, were prominent. Gliosis was still apparent but became progressively weaker. In summary, the combined histological and *in situ* hybridization data indicate that standard MV as well as MV-ΔM spread through the brain, attesting that M protein is dispensable for spreading in the CNS. Nevertheless, the pathogenicity and mode of propagation of MV-ΔM were characteristically different from those of standard MV, and similar to those of MV-Δ_{tails}.

Discussion

It is shown here that M, a major MV structural protein, is not absolutely required for virus spread. Remarkably, an M-less MV switches mode of propagation: whereas formation of cell-free infectivity is very inefficient, fusion of MV-ΔM infected cells with neighbouring cells is enhanced. Consistent with this, the highly fusogenic/assembly-defective M-less virus propagates more deeply in the brain parenchyma of genetically modified mice than standard MV.

M protein function: virus assembly

The M protein of paramyxoviruses is believed to play a central role in virus assembly by coordinating the interactions of the viral components and the cytoskeleton at internal cell membranes (Peeples, 1991; Sanderson *et al*., 1995). Assembly is completed beneath the plasmalemma, from whence particles bud. In cultured cells, production of infectious particles is considerably less efficient for

MV than for other paramyxoviruses: on the one hand, under optimal conditions 50 cell-associated and five cell-free infectious particles/cell can be recovered (Udem, 1984; Cattaneo *et al*., 1987); on the other hand, more numerous cell-associated particles can be visualized by electron microscopy (Bohn *et al*., 1983; Figure 4).

In the parallel standard MV infections of Figure 2G an average of seven cell-associated infectious particles per cell were formed, and fewer than one per cell was released. In MV-ΔM infections only one infectious unit per 40 cells was formed, and one per 500 cells was released (Figure 2H). Biochemical characterization of MV-ΔM infectivity was attempted using methods applied to the analysis of standard, altered or chimeric MV particles (Cathomen *et al.*, 1998; Spielhofer *et al*., 1998) but failed. This may be due in part to the limited amount of material available, and in part to heterogeneity or fragility of the infectivity (see below). However, by electron-microscopy virus-like MV-ΔM particles were monitored in the vicinity of infected syncytia, but only rarely did these particles contain ribonucleocapsid-like filaments (Figure 4F and G). Considering these facts we refer to MV-ΔM 'infectious units' or 'infectivity' rather than to MV-ΔM 'infectious particles'.

MV-ΔM infectivity may consist of plasmalemma vesicles containing viral glycoproteins and ribonucleocapsids. The production of these infectious vesicles may be favoured by the fact that even without M protein the viral glycoproteins partly retain clustering in membrane microdomains (Figures 3 and 4). These microdomains may be extruded stochastically from cells based on constitutive exocytotic mechanisms. At late infection stages, when all viral components are present at high concentrations, a fraction of these glycoprotein-enriched vesicles would contain ribonucleocapsids and behave as infectivity. A precedent for the formation of infectious, membrane-enveloped vesicles is available: the RNA of a Semliki forest virus-derived replicon encoding the vesicular stomatitis virus glycoprotein is encapsidated in glycoprotein-enriched particles and propagates at low titres in cultured cells (Rolls *et al*., 1994).

We conclude that in the absence of M, orthodox MV particles cannot be formed, as expected. Unexpectedly however, MV-ΔM infections propagate as efficiently as standard infections in cultured cells, on the basis of enhanced cell-to-cell fusion.

An M protein function in fusion control?

Can the more extensive fusion of MV-ΔM-infected cells be explained simply by extensive accumulation of viral glycoproteins on the surface due to the lack of virus budding? Probably not, because even in standard MV infections budding is inefficient. Consistent with this, the half-life of the MV glycoproteins on the cell surface is long (~10 h; Fujinami *et al*., 1981) and the stability of fully processed H proteins in standard infections and MV-ΔM infections is similar (Figure 1C and data not shown). Similarly, an altered distribution of the viral envelope proteins on the cell surface is unlikely to account for enhanced cell fusion: MVs with altered envelope protein cytoplasmic tails maintain a completely patchy distribution of the envelope proteins but induce enhanced cell-to-cell fusion (Cathomen *et al.*, 1998). As a third rationale it could be argued that MV-ΔM particles may contain many more genomes than standard MV particles. In this case MV-ΔM infections would have a head start, and the MV-ΔM syncytia would always appear larger. Two observations dismiss this possibility: first, even in infections starting from genomic plasmids MV-ΔM syncytia appear earlier than standard MV syncytia. Secondly, MV-ΔM syncytia are qualitatively different: they maintain a more regular organization of the nuclei and grow to a larger size before loosing attachment (T.Cathomen, unpublished data).

We suggest that the association of M with the cytoplasmic tails of the glycoproteins may negatively influence their fusion efficiency (Cathomen *et al*., 1998). Indeed, a fusion regulatory function of the M protein was proposed based on the analysis of an MV strain composed of a non-resolvable mixture of highly productive, non-fusogenic MV and a cell-associated, highly fusogenic virus (Carrigan, 1985). Moreover, electron microscopy observations of two other paramyxoviruses are consistent with an M-protein-imparted fusion-refractory state of the envelope protein complex (Buechi and Bächi, 1982; Russell and Almeida, 1984).

Interestingly, a fusion-regulatory function of the human immunodeficiency virus (HIV) M protein has been postulated on the basis of genetic data (De Mareuil *et al*., 1995). Remarkably, HIV-1 variants with truncated cytoplasmic tails are more fusogenic than standard viruses (Wilk *et al*., 1992). Moreover, removal of a short segment from the cytoplasmic tail of the envelope protein of two other retroviruses enhances the competence of these envelope proteins for fusion (Brody *et al*., 1992; Januszeski *et al*., 1997). Obviously the functions of the matrix proteins of paramyxoviruses and retroviruses cannot be compared directly, but it can be noted that all viruses fusing at neutral pH may have to regulate fusion competence in order to prevent immediate re-infection upon virus release and to limit fusion of intracellular membranes. This problem does not exist for viruses entering the cell via the endocytic vacuolar system, where fusion is activated by acidic pH (Helenius, 1995; Hernandez *et al*., 1996).

Brain propagation of mutated MV and SSPE

We examined the propagation of the M-less, cell-free, highly fusogenic MV in the brain of adult mice expressing CD46 with human-like tissue specificity and defective for the interferon type I receptor (Mrkic *et al*., 1998). Not only MV-ΔM and standard MV, but also an engineered MV with altered F and H glycoprotein cytoplasmic tails (MV-Δ_{tails}) were tested. This virus exhibits increased cell-to-cell fusion competence but produces particles at lower levels than standard MV (Cathomen *et al.*, 1998). Both MV-ΔM and MV-Δ_{tails} penetrated more deeply than standard virus into the brain parenchyma. Thus the gain in cell-to-cell fusion competence of assembly-defective viruses also appears to contribute to the spread of infectivity in brain. The situation may be similar in persistent MV infections of human brains: mutated, assembly-defective MV do overgrow parental virus (Schmid *et al*., 1992; Baczko *et al*., 1993). However, it must be emphasized that the short-term infections of mouse brain differ profoundly from SSPE, which develops over several years in humans.

The histological analysis of brains from mice inoculated with low doses of standard MV sacrificed days or weeks

p.i. is of interest: viral replication and inflammatory lesions were observed in different parts of the parenchyma close to regions contacting the cerebrospinal fluid. In particular, in one of these areas, the hippocampal CA1 region, a characteristic nerve cell loss was monitored. Remarkably, a similar pathology was described previously in adult BALB/c mice infected with neurotropic MV strains (Andersson *et al*., 1993; Eastman *et al*., 1994) and in newborn hamsters (Carrigan, 1986). In contrast, MV-ΔM or MV-Δ_{tails} infections did not induce this pathogenic feature but penetrated more deeply than standard virus in the brain parenchyma. It can be speculated that the destruction of a whole specialized area of the CNS may be lethal, whereas patchy, partial destruction of many areas can be overcome.

An hypothetical scenario of MV propagation in human brain may be as follows. After acute respiratory infection and systemic spread, in a significant fraction of cases MV may invade the CNS and replicate (ter Meulen *et al*., 1983; Katayama *et al*., 1995). Whereas standard MVs can be efficiently eliminated by the host immune system (Carrigan, 1986), assembly-defective MVs may be better tolerated and thus persist more often. These viruses, being highly fusogenic, would propagate deep in the brain parenchyma. In most cases, the spread of these viruses may be limited and thus asymptomatic, as in MV-ΔM- and MV-Δ_{tails}-infected mouse brains. However, in an exceedingly low percentage of infected human brains continuous virus spread may cause progressive impairment of function, which will slowly lead first to SSPE and then to death.

Materials and methods

Plasmid constructions

Plasmid p(+)MV-ΔM containing the full-length antigenomic copy of the M-gene-deficient MV genome was constructed in two steps: after excision of a *Bgl*II–*Bcl*I fragment containing 960 nucleotides of the M-gene-coding region from plasmid pePMF2 (R.Cattaneo, unpublished), plasmid fragments were religated giving rise to pePΔMF2 (Figure 1A). Plasmid p(+)MV-ΔM was obtained by three-way ligation of a *Sac*II–*Nar*I fragment of pePΔMF2 with a *Nar*I–*Pac*I and the *Pac*I–*Sac*II fragment of p(+)MV (Radecke *et al*., 1995) containing the terminal MV genome segments and the plasmid backbone.

Viruses and virus assays

MV-ΔM rescued from p(+)MV-ΔM, the standard tagged MV derived from the Edmonston-B-based plasmid p(+)MV, and MV-Δ_{tails} were propagated and purified as described previously (Radecke *et al*., 1995). The biological activities of the viruses were determined by plaque assays (Radecke *et al*., 1995) or by 50% end-point dilution assays ($TCID_{50}$; Cathomen *et al*., 1998).

RT–PCR

For RNA analysis, infected Vero cells were lysed and total RNA isolated using RNeasy spin columns (Qiagen). Reverse transcription was performed with M-MLV reverse transcriptase (Gibco-BRL) using specific primers binding to the 3′-terminal region of either the M gene or the N gene, respectively. For amplification of the M gene, primers annealing to both gene ends were used, for amplification of the N gene primers whose 5′-end is situated 475 nucleotides apart were used.

Metabolic labelling, immunoprecipitation and endo H digestion

Metabolic labelling, immunoprecipitation and endo H digestion were performed as previously described (Cattaneo and Rose, 1993). Briefly, Vero cells were infected with MV or MV-ΔM at an m.o.i. of 0.5 for 2 h at 37°C. Sixteen hours p.i., cells were starved for 30 min in methionine/cysteine-free Dulbecco's modified Eagle's medium (DMEM), pulsed for 1 h in the presence of 100 μCi Tran^{35}S-label (ICN) and, if indicated, chased for 4 h with DMEM supplemented with 10% fetal calf serum (DMEM-10). Immunoprecipitation was performed using a polyclonal goat anti-MV antibody (courtesy of S.Udem).

Growth analysis

Vero cells (2×10^5) in 15 mm wells were infected with MV or MV-ΔM at an m.o.i. of 0.01 for 2 h at 37°C. Inocula were collected to control virus adsorption. Cells were washed twice with phosphate-buffered saline (PBS), overlain with 500 μl DMEM-5 and incubated at 32.5°C to favour virus release (Udem, 1984). Every 24 h cell-free and cell-associated virus were collected and stored at –30°C. Cell-free samples were prepared by clarifying supernatants of infected cells for 2 min at 8000 r.p.m. in an Eppendorf centrifuge. Cell-associated virus was recovered by scraping infected cells into 500 μl DMEM-5. Infectivity was determined by $TCID_{50}$ titration.

Confocal microscopy

Infected Vero cells on glass cover-slips were double-labelled for M and H or P and H protein. After fixation in methanol and blocking in 0.5% bovine serum albumin (BSA) in PBS, cells were incubated with antibodies diluted in PBS containing 0.5% Tween-20. The primary antibody mixtures contained either a monoclonal anti-M or anti-P antibody (both 1:200; courtesy of C.Örvell) and a rabbit anti-peptide serum against H (1:200; Buchholz *et al*., 1996). The secondary antibody mixture consisted of an FITC-conjugated donkey anti-mouse IgG and a donkey anti-rabbit IgG coupled to TRITC (both 1:100; Jackson). Cover-slips were mounted using the antifadant Citifluor AF1 (Cancer Research Campaign) and immunoreactivity was visualized using confocal microscopy (Leica TCS NT) in conjunction with a Leitz DM IRBE fluorescence microscope in ~0.4 μm optical sections. Image stacks, confirmed by single excitation to prevent spill-over artefacts, were obtained in double-excitation mode and recombined using Imaris and Selima image-processing software (Bitplane AG, Technopark Zurich, Switzerland).

Electron microscopy

Vero cells in 24-well culture dishes were infected with MV or MV-ΔM at an m.o.i. of 0.05. After 2 days incubation at 32.5°C (syncytia formation involved ~90% of the cells), the culture medium was removed and cells were fixed for 1 h in 4% paraformaldehyde made in cacodylate buffer. The cells were then rinsed three times in PBS and blocked for 30 min in PBS containing 5% acetylated bovine serum albumin (BSAc, Aurion, The Netherlands), 0.1% cold-water fish skin gelatine and 1% normal goat serum. After three washes in PBS containing 0.1% BSAc (PBS–BSAc), cells were incubated overnight at 4°C in a humid chamber with a pool of monoclonal antibodies (courtesy of D.Gerlier) against either H or F (diluted 1:1000 in PBS–BSAc). Cells were washed three times in PBS–BSAc and then incubated at 4°C for 4 h with goat anti-mouse antibodies coupled to 10-nm colloidal gold particles (1:40; Aurion). After washing three times in PBS–BSAc and five times in PBS, the cells were fixed consecutively in 2% glutaraldehyde made in PBS, 0.5% osmium tetroxide and 2% uranyl acetate. Samples were then dehydrated stepwise with increasing concentrations of ethanol and embedded in epon. After polymerization the samples were cut into 100 nm thick sections, recovered onto copper grids, stained with uranyl acetate and lead citrate and then analysed under a Philips CM120 Biotwin electron microscope at 120 kV.

Histopathology and in situ hybridization

Histopathology and *in situ* hybridization were basically performed as described elsewhere (Mrkic *et al*., 1998). Briefly, for histopathological analysis mice were sacrificed and the brains fixed in 4% PBS-buffered formaldehyde. Sagittal and coronal brain sections were cut at 2 μm and either stained with haematoxylin/eosin or luxol/fast nuclear red or prepared immunohistochemically with rabbit anti-GFAP antibodies followed by detection with avidin–biotin–peroxidase (VectorLabs). MV N-specific mRNA was detected in brain sections with DIG-labelled antisense N mRNA probes. Immunological detection and staining was performed using a DIG nucleic acid detection kit (Boehringer Mannheim).

Acknowledgements

We thank Frank Radecke for help with the infectious cDNA system, Gudrun Christiansen, Marianne König, Norbert Wey and Fritz Ochsenbein for excellent technical assistance, Denis Gerlier, Clas Örvell and Steve Udem for antibody gifts, and Charles Weissmann, Ueli

Suter, Hussein Naim, Karl-Klaus Conzelmann and Michael A.Klein for discussions and comments on the manuscript. This work was supported by grants of the Swiss National Science Foundation to R.Cattaneo. The Swiss Serum and Vaccine Institute provided the salary of B.M.

References

Andersson,T., Schwarcz,R., Love,A. and Kristensson,K. (1993) Measles virus-induced hippocampal neurodegeneration in the mouse: a novel, subacute model for testing neuroprotective agents. *Neurosci. Lett.*, **154**, 109–112.

Baczko,K. *et al.* (1993) Clonal expansion of hypermutated measles virus in a SSPE brain. *Virology*, **197**, 188–195.

Billeter,M.A. and Cattaneo,R. (1991) Molecular biology of defective measles virus persisting in the human central nervous system. In Kingsbury,D.W. (ed.), *The Paramyxoviruses*. Plenum Press, New York, pp.323–345.

Bohn,W., Rutter,G., Hohenberg,H. and Mannweiler,K. (1983) Inhibition of measles virus budding by phenothiazines. *Virology*, **130**, 44–55.

Brody,B.A., Rhee,S.S., Sommerfelt,M.A. and Hunter,E. (1992) A viral protease-mediated cleavage of the transmembrane glycoprotein of Mason–Pfizer monkey virus can be suppressed by mutations within the matrix protein. *Proc. Natl Acad. Sci. USA*, **89**, 3443–3447.

Buchholz,C.J., Schneider,U., Devaux,P., Gerlier,D. and Cattaneo,R. (1996) Cell entry by measles virus: long hybrid receptors uncouple binding from membrane fusion. *J. Virol.*, **70**, 3716–3723.

Buechi,M. and Bächi,T. (1982) Microscopy of internal structures of Sendai virus associated with the cytoplasmic surface of host membranes. *Virology*, **120**, 349–359.

Carrigan,D.R. (1985) Round cell variant of measles virus: spontaneous conversion from productive to cell-associated state of infection. *Virology*, **144**, 337–350.

Carrigan,D.R. (1986) Round cell variant of measles virus: neurovirulence and pathogenesis of acute encephalitis in newborn hamsters. *Virology*, **148**, 349–359.

Cathomen,T., Naim,H.Y. and Cattaneo,R. (1998) Measles viruses with altered envelope protein cytoplasmic tails gain cell fusion competence. *J. Virol.*, **72**, 1224–1234.

Cattaneo,R. and Rose,J.K. (1993) Cell fusion by the envelope glycoproteins of persistent measles viruses which caused lethal human brain disease. *J. Virol.*, **67**, 1493–1502.

Cattaneo,R., Rebmann,G., Schmid,A., Baczko,K. and Billeter,M.A. (1987) Altered transcription of a defective measles virus genome derived from a diseased human brain. *EMBO J.*, **6**, 681–688.

Cattaneo,R., Schmid,A., Eschle,D., Baczko,K., ter Meulen,V. and Billeter,M.A. (1988) Biased hypermutation and other genetic changes in defective measles viruses in human brain infections. *Cell*, **55**, 255–265.

De Mareuil,J., Salaun,D., Chermann,J.C. and Hirsch,I. (1995) Fusogenic determinants of highly cytopathic subtype D Zairian isolate HIV-1NDK. *Virology*, **209**, 649–653.

Eastman,C.L., Urbanska,E., Love,A., Kristensson,K. and Schwarcz,R. (1994) Increased brain quinolinic acid production in mice infected with a hamster neurotropic measles virus. *Exp. Neurol.*, **125**, 119–124.

Fujinami,R.S., Sissons,J.G.P. and Oldstone,M.B.A. (1981) Immune reactive measles virus polypeptides on the cell's surface: turnover and relationship of the glycoproteins to each other and to HLA determinants. *J. Immunol.*, **127**, 935–940.

Griffin,D.E. and Bellini,W.J. (1996) Measles virus. In Fields,B.N., Knipe, D.M. and Howley,P.M. (eds), *Virology*. Raven, Philadelphia, PA, pp. 1267–1312.

Helenius,A. (1995) Alphavirus and flavivirus glycoproteins: structures and functions. *Cell*, **81**, 651–653.

Hernandez,L.D., Hoffman,L.R., Wolfsberg,T.G. and White,J.M. (1996) Virus–cell and cell–cell fusion. *Annu. Rev. Cell Dev. Biol.*, **12**, 627–661.

Hirano,A., Ayata,M., Wang,A.H. and Wong,T.C. (1993) Functional analysis of matrix proteins expressed from cloned genes of measles virus variants that cause subacute sclerosing panencephalitis reveals a common defect in nucleocapsid binding. *J. Virol.*, **67**, 1848–1853.

Januszeski,M.M., Cannon,P.M., Chen,D., Rozenberg,Y. and Anderson,W.F. (1997) Functional analysis of the cytoplasmic tail of moloney murine leukemia virus envelope protein. *J. Virol.*, **71**, 3613–3619.

Katayama,Y., Hotta,H., Nishimura,A., Tatsuno,Y. and Homma,M. (1995) Detection of measles virus nucleoprotein mRNA in autopsied brain tissues. *J. Gen. Virol.*, **76**, 3201–3204.

Kristensson,K. and Norrby,E. (1986) Persistence of RNA viruses in the central nervous system. *Ann. Rev. Microbiol.*, **40**, 159–184.

Liebert,U.G. and Finke,D. (1995) Measles virus infections in rodents. In ter Meulen,V. and Billeter,M.A. (eds), *Measles Virus*, Vol. 191. Springer-Verlag, Berlin, Germany, pp.149–166.

Mrkic,B., Pavlovic,J., Rülicke,T. Volpe,P. Buchholz,C.J., Hourcade,D. Atkinson,J.P. Aguzzi,A. and Cattaneo,R. (1998) Measles virus spread and pathogenesis in genetically modified mice. *J. Virol.*, **72**, in press.

Peeples,M.E. (1991) Paramyxovirus M proteins. Pulling it all together and taking it on the road. In Kingsbury,D.W. (ed.), *The Paramyxoviruses*. Plenum Press, New York, pp. 427–456.

Radecke,F., Spielhofer,P., Schneider,H., Kaelin,K., Huber,M., Dötsch,C., Christiansen,G. and Billeter,M.A. (1995) Rescue of measles viruses from cloned DNA. *EMBO J.*, **14**, 5773–5784.

Rall,G.F., Manchester,M., Daniels,L.R., Callahan,E.M., Belman,A.R. and Oldstone,M.B.A. (1997) A transgenic mouse model for measles virus infection of the brain. *Proc. Natl Acad. Sci., USA*, **94**, 4659–4663.

Rolls,M.M., Webster,P., Balba,N.H. and Rose,J.K. (1994) Novel infectious particles generated by expression of the vesicular stomatitis virus glycoprotein from a self-replicating RNA. *Cell*, **79**, 497–506.

Russell,P.H. and Almeida,J.D. (1984) A regular subunit pattern seen on non-infectious Newcastle disease virus particles. *J. Gen. Virol.*, **65**, 1023–1031.

Sanderson,C.M., Avalos,R., Kundu,A. and Nayak,D.P. (1995) Interactions of Sendai viral F, HN and M proteins with host cytoskeletal and lipid components in Sendai-virus infected BHK cells. *Virology*, **209**, 701–707.

Schmid,A., Spielhofer,P., Cattaneo,R., Baczko,K., ter Meulen,V. and Billeter,M.A. (1992) Subacute sclerosing panencephalitis is typically characterized by alterations in the fusion protein cytoplasmic domain of the persisting measles virus. *Virology*, **188**, 910–915.

Spielhofer,P., Bächi,T., Fehr,T., Christiansen,G., Cattaneo,R., Kaelin,K., Billeter,M.A. and Naim,H.Y. (1998) Chimeric measles viruses with a foreign envelope. *J.Virol.*, **72**, 2150–2159.

ter Meulen,V., Stephenson,J.R. and Kreth,H.W. (1983) Subacute sclerosing panencephalitis. In Fraenkel-Conrat,H. and Wagner,R.R. (eds), *Virus–Host Interactions: Receptors, Persistence and Neurological Diseases*, Vol. 18. Plenum Press, New York, pp. 105–159.

Udem,S.A. (1984) Measles virus: conditions for the propagation and purification of infectious virus in high yield. *J. Virol. Meth.*, **8**, 123–136.

van Binnendijk,R.S., van der Heijden,R.W.J. and Osterhaus,A.D.M.E. (1995) Monkeys in measles research. In ter Meulen,V. and Billeter,M.A. (eds), *Measles Virus*, Vol. 191. Springer-Verlag, Berlin, Germany, pp.135–148.

Wilk,T., Pfeiffer,T. and Bosch,V. (1992) Retained *in vitro* infectivity and cytopathogenicity of HIV-1 despite truncation of the C-terminal tail of the env gene product. *Virology*, **189**, 167–177.

Received April 27, 1998; accepted May 19, 1998